

Article

Pull-Out Capability of a 3D Printed Threadless Suture Anchor with Rectangular Cross-Section: A Biomechanical Study

Yueh-Ying Hsieh ^{1,2}, Lien-Chen Wu ^{1,2,3}, Fon-Yih Tsuang ⁴ , Chia-Hsien Chen ^{1,2,3} and Chang-Jung Chiang ^{1,2,*} 

¹ Department of Orthopedics, Shuang Ho Hospital, Taipei Medical University, New Taipei City 23561, Taiwan; 11154@s.tmu.edu.tw (Y.-Y.H.); d98548019@tmu.edu.tw (L.-C.W.); chiaxian@tmu.edu.tw (C.-H.C.)

² Department of Orthopaedics, School of Medicine, College of Medicine, Taipei Medical University, Taipei City 110, Taiwan

³ Graduate Institute of Biomedical Materials and Tissue Engineering, College of Biomedical Engineering, Taipei Medical University, Taipei City 110, Taiwan

⁴ Division of Neurosurgery, Department of Surgery, National Taiwan University Hospital, Taipei City 110, Taiwan; tsuangfy@ntu.edu.tw

* Correspondence: cjchiang@s.tmu.edu.tw

Abstract: Suture anchor fixation is a common method for securing bone and soft tissue in the body, with proven applications in the hip, elbow, hand, knee and foot. A critical limiting factor of suture anchors is the pull-out strength, particularly in suboptimal bone. This study introduces a novel 3D printed threadless suture anchor with a rectangular cross-section. The titanium anchor was designed with surface fenestration and a porous central core to improve bone ingrowth. The aim of this study was to compare the pull-out properties of the novel threadless anchor with a traditional circular threaded suture anchor. The anchors were inserted into a 0.24 g/cm³ synthetic cancellous bone block at angles of 90° and 135° to the surface. The sutures were pulled at 180° (parallel) to the surface under a static pull test (anchor pullout) and cyclic load test using a tensile testing machine. Under the static load, the greatest pullout strength was seen with the novel threadless anchor inserted at 90° (mean, 105.6 N; standard deviation [SD], 3.5 N). The weakest pullout strength was seen with the threaded anchor inserted at 90° (mean, 87.9 N; SD, 4.1 N). In the cyclic load test, all six of the threaded anchors with a 90° insertion angle pulled out after 18 cycles (70 N). All of the threadless anchors inserted at 90° survived the cyclic test (90 N). In conclusion, the novel threadless suture anchor with rectangular cross-section and traditional threaded suture anchor had similar pullout survivorship when inserted at either 90° or 135°. In addition, the 3D printed threadless anchor has the potential for good bone integration to improve long-term stabilization.



Citation: Hsieh, Y.-Y.; Wu, L.-C.; Tsuang, F.-Y.; Chen, C.-H.; Chiang, C.-J. Pull-Out Capability of a 3D Printed Threadless Suture Anchor with Rectangular Cross-Section: A Biomechanical Study. *Appl. Sci.* **2021**, *11*, 12128. <https://doi.org/10.3390/app112412128>

Academic Editor: Claudio Belvedere

Received: 21 October 2021

Accepted: 17 December 2021

Published: 20 December 2021

Publisher's Note: MDPI stays neutral with regard to jurisdictional claims in published maps and institutional affiliations.



Copyright: © 2021 by the authors. Licensee MDPI, Basel, Switzerland. This article is an open access article distributed under the terms and conditions of the Creative Commons Attribution (CC BY) license (<https://creativecommons.org/licenses/by/4.0/>).

Keywords: suture anchor; threadless; pull-out capability; 3D printing; biomechanical study

1. Introduction

Fixation with suture anchors is a common method of securing bone and soft tissue during orthopedic surgery, and is particularly prevalent in endoscopic surgery. Various designs of suture anchor have been proposed, including different materials, shapes and sizes, with the intent of ensuring a secure fixation between the soft tissue and bone until healing is complete [1–3]. Although metallic suture anchors with nonabsorbable sutures are routinely used and provide a good initial fixation, clinical studies have reported anchor-associated complications such as migration, loosening, breakage, and interference from surrounding tissues [4,5].

Djurasovic et al. [6] reported that 10% of fixation failures with suture anchors used for rotator repair are associated with anchor loosening or migration. However, early bone healing around the anchor may increase the pull-out strength and reduce migration or loosening. Thus, 3D printing allows for the rapid development of hollow or perforated structures which can be tailored to different orthopedic applications to improve bone

ingrowth. MacBarb et al. [7] designed a perforated 3D printed structure with a porous outer surface which demonstrated good bone ingrowth when implanted in an ovine model. In a 24-month follow-up study, Patel et al. [8] reported no cases of implant breakage, migration or subsidence in 51 sacroiliac joint fusion cases when using 3D-printed triangular titanium implants. Wei et al. [9] used 3D-printed technology to develop a suture anchor with barbs and their results indicated that the 3D-printed technology could make the anchor maximum strength to hold reshaped tissue structures.

Progressing previous research on a 3D-printed triangular titanium implant [7], our research team developed a novel 3D-printed titanium suture anchor with rectangular cross-section, surface fenestration and a porous central core. When compared to the circle cross-section implant, the rectangular cross-section shape minimizes rotation by the press-fit with four corners. Moreover, the structural fenestrations and porous structure (70% porosity and 600 μm pore size) allow for bone ingrowth to the central core, leading to permanent fixation. When inserted into a predrilled round hole, the surface roughness of the implant and friction generated between the implant and bone allow for a press-fit insertion, removing the need for a threaded outer surface for initial fixation strength. The press-fit action also forces surrounding cancellous bone into the pores and fenestrations. The small footprint of our anchor also allows for more bone stock to be preserved, which is highly beneficial in cases of revision surgery [10]. In comparison with the traditional thread suture anchor with circle cross-section our design concept is to provide higher anti-rotation ability, a smaller footprint, porous structure allows for bony on growth and ingrowth.

Pull-out testing gives a good indicator of initial purchase strength after implantation, and is a critical step when designing novel implants. The pullout test consists of applying a tensile force until the anchor pulls out of the substrate, with the maximum force generated being taken as the pull-out force. Loading is typically applied at 0° , 90° , and 135° relative to the long-axis of anchor, however, a loading angle of 0° is not commonly experienced by suture anchors in vivo [11–13]. Nagamoto et al. [14] indicated that the pull-out strength of a threadless anchor was greatest when loading was applied at 90° .

It is difficult to directly compare fixation techniques in cadavers and animal models due to variations in bone quality, bone anatomy, and fixation location. Hence, the purpose of this study is to compare the pull-out properties of a threadless rectangular suture anchor and a traditional threaded suture anchor when inserted in a synthetic testing block at 90° and 135° , simulating common in vivo insertion angles.

2. Materials and Methods

This study aimed to replicate implantation in a healthy human humerus. To achieve this, synthetic sawbones (Sawbones, Pacific Research Laboratories, Vashon, WA, USA) were used which had a similar density (0.24 g/cm^3 , 15 PCF, solid polyurethane foam) to the greater tuberosity [15,16]. The sawbones were shaped into sample blocks of size $60 \text{ mm} \times 40 \text{ mm} \times 40 \text{ mm}$ ($W \times D \times H$). Two types of suture anchors were assessed in this study; (i) threaded titanium anchor, outer diameter 3.5 mm and 10 mm in length (TwinFix™ Ti 3.5, Smith & Nephew, Andover, MA, USA), and (ii) a custom-made, 3D printed titanium alloy suture anchor of size $2.5 \text{ mm} \times 2.5 \text{ mm} \times 10 \text{ mm}$ ($W \times D \times H$) with rectangular cross-section and surface fenestration (Figure 1). The anchors were modeled in Creo 2.0 (PTC, Boston, MA, USA) and these 3D CAD models were used to print the anchors using EOS Titanium Ti64ELI powder on an EOS M290 Selective Laser Melting Metal Additive Manufacturing Machine (EOS GmbH, Krailling, Germany). The following machine parameters recommended by the equipment manufacturer were used: laser power of 280 W, scan speed of 1200 mm/s, resolution of 0.02 mm, and layer thickness of 30 μm .

The sawbone samples were held in a custom jig and a pilot hole of diameter 2.5 mm and depth 10 mm drilled in each. Each anchor was inserted at angles of 90° and 135° from the surface of the sawbone to the same depth (Figure 2). The aim of this study was to compare the pull-out properties of different anchors, and so braided polyethylene sutures were used for all tests to negate the potential influence of different suture materials or

designs. The sutures were hand-tied around the pulling jig with a single surgeon's knot and four square knots [17]. A universal testing machine (eXpert 3910, ADMET, UK) equipped with a custom-made pulling jig was used to perform the pullout tests (Figure 3). Each anchor was preloaded with a 10 N force applied at 1 mm/s at an angle of 180° (parallel) to the surface to ensure sufficient contact between the implant and bone [15,18]. This preloading stage was immediately followed by the pull-test in the static model with the load being applied at a rate of 1 mm/s. The fixation strength of each anchor was defined by the maximum load recorded prior to failure by any means. Each test setup was performed 6 times with separate anchors and separate sawbone samples. Six constructs were tested for each insertion angle. The stiffness of each anchor was determined through linear regression modelling of the force-displacement curve for each construct ranging from 20–80% of the ultimate load [17]. A one-tailed t test model with a significance level (α) of 0.05 was used.

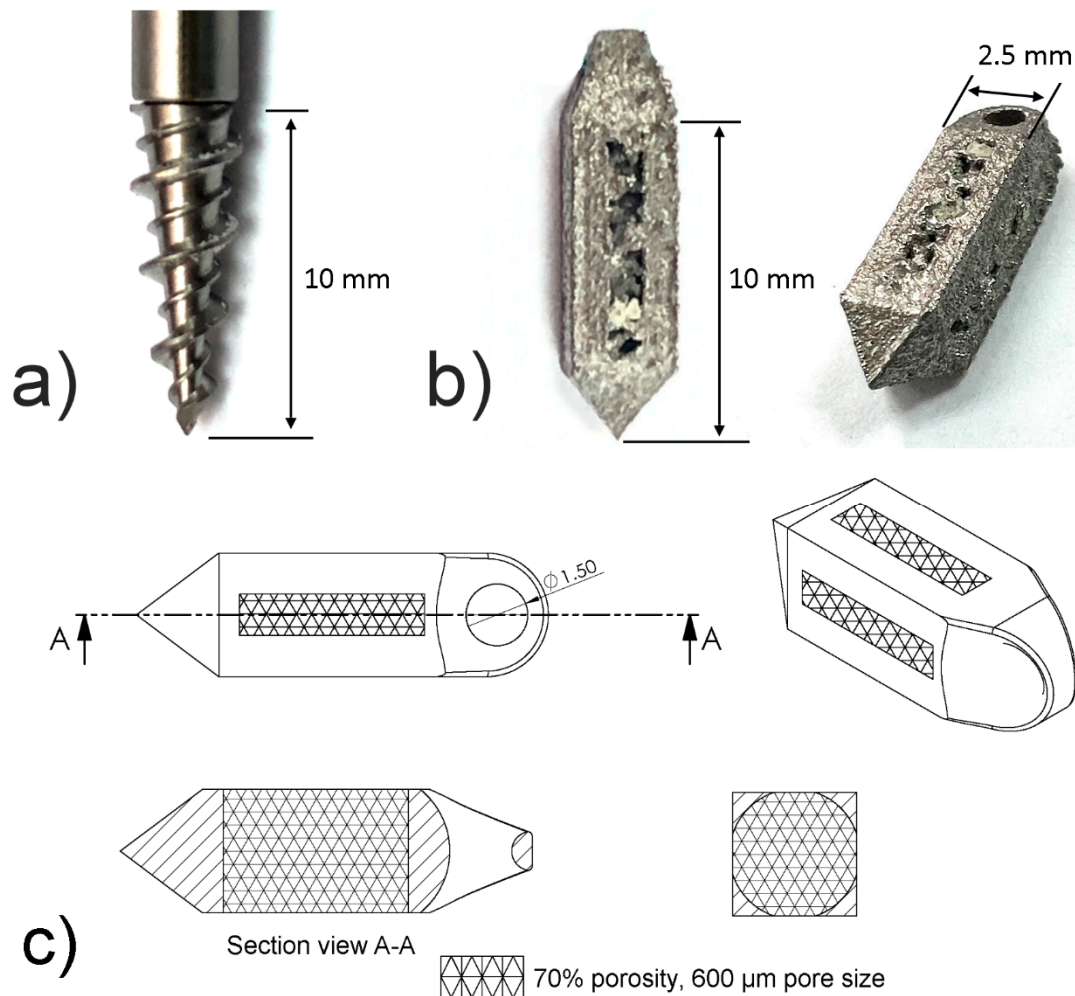


Figure 1. (a) Commercially-available threaded suture anchor (TwinFix™ Ti 3.5, Smith & Nephew, Andover, MA, USA); (b) custom-made threadless suture anchor with rectangular cross-section; (c) design drawing of the custom-made threadless suture anchor.

Cyclic testing was performed in accordance with the protocol devised by Clevenger et al. [17]. Each specimen was cycled from 0 to 50 N for 10 cycles, from 0 to 70 N for 10 cycles, and from 0 to 90 N for 10 cycles, up to a maximum of 30 cycles at a rate of 1 Hz. The number of cycles required to induce complete anchor pullout was recorded.

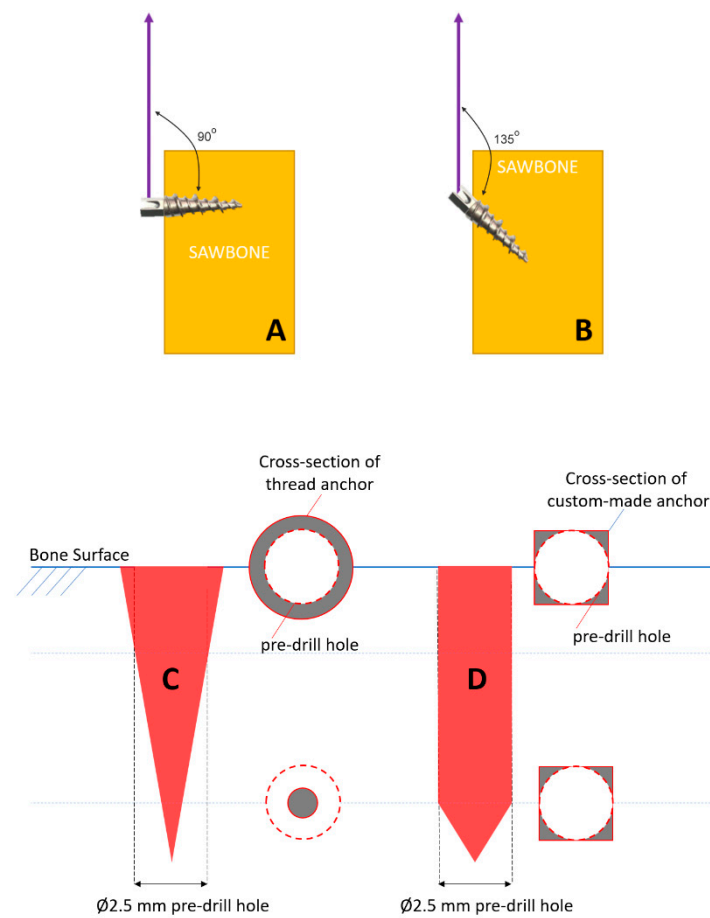


Figure 2. Loading was applied at 180° (parallel) to the bone surface. (A) Anchor inserted at 90° from the bone surface. (B) Anchor inserted at 135° from the bone surface. (C) Contact surface between threaded suture anchor and pre-drilled hole. (D) Contact surface between custom-made suture anchor and pre-drilled hole.



Figure 3. Experimental setup. The sawbone was clamped in place and the braided polyethylene lines were tied to a custom-made pulling jig.

3. Results

In the static test all constructs failed through screw pullout. Table 1 and Figure 4 detail the strength and stiffness of both suture anchors. The threadless suture anchor with 90° insertion angle had the greatest fixation strength of all test setups, having a mean pullout strength of 105.6 N (standard deviation [SD], 3.5 N) and mean stiffness of 65.2 N/mm (4.3). There was a statistically significant difference in failure load and stiffness between the two groups when inserted at 90° (Figure 4).

Table 1. Mean pullout strength and stiffness for each group.

	Mean Pullout Strength N, (SD)		Mean Pullout Stiffness N/mm, (SD)	
	90° Insertion Angle	135° Insertion Angle	90° Insertion Angle	135° Insertion Angle
Thread metallic suture anchor	87.9 (4.1)	96.8 (4.3)	31.3 (2.3)	64.9 (5.3)
Custom-made suture anchor	105.6 (3.5)	92.9 (4.5)	65.2 (4.3)	58.6 (5.9)

■ Thread metallic anchor
 ■ Custom-made anchor

* $p < 0.05$

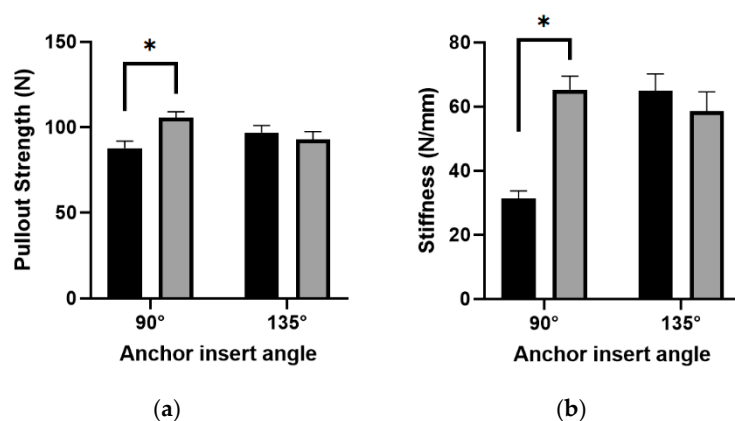


Figure 4. (a) Mean load to failure, showing a significant difference ($p < 0.05$) between the groups with a 90° insertion angle.; (b) mean construct stiffness, showing a significant difference ($p < 0.05$) between the groups with a 90° insertion angle.

In the cyclic test (Table 2 and Figure 5), all 6 threaded suture anchors inserted at 90° pulled out after 18 cycles, and 5 of the threaded anchors inserted at 135° pulled out after 25 cycles. In the threadless group, all suture anchors with a 90° insertion angle survived the full 30 cycles, while all 6 anchors inserted at 135° pulled out after 22 cycles.

Table 2. Percentage of specimens intact (survived) after cyclic testing.

	90° Insertion Angle			135° Insertion Angle		
	Cycle No.	Cycled force (N)	Survived (%)	Cycle No.	Cycled force (N)	Survived (%)
Thread metallic suture anchor	1 to 10	0 to 50	100%	1 to 10	0 to 50	100%
	11 to 20	0 to 70	67%	11 to 20	0 to 70	100%
	21 to 30	0 to 90	0%	21 to 30	0 to 90	17%
Custom-made suture anchor	1 to 10	0 to 50	100%	1 to 10	0 to 50	100%
	11 to 20	0 to 70	100%	11 to 20	0 to 70	100%
	21 to 30	0 to 90	100%	21 to 30	0 to 90	0%

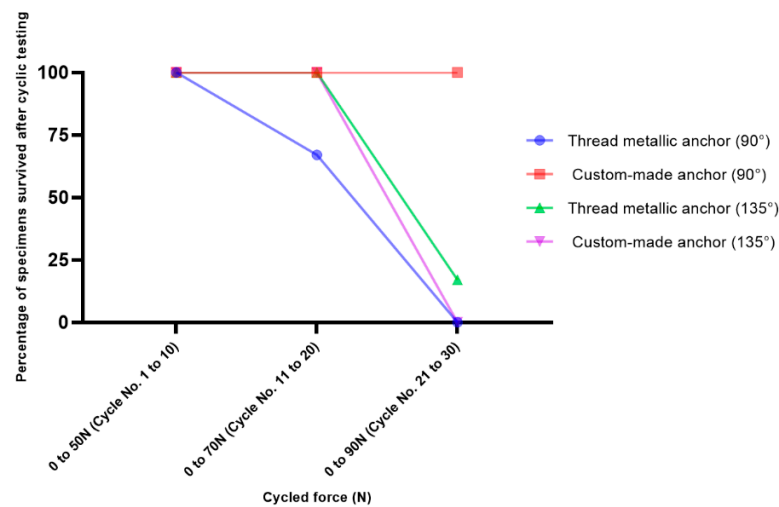


Figure 5. Compared to different insertion angle, cycled force and cycle numbers of survival proportions.

There were no metal particles loosely adhered to the anchors after static and cyclic tests.

4. Discussion

Failure of suture anchors at the bone–anchor interface, such as through pullout, is not uncommon, especially in elderly osteoporotic patients. The fixation ability is adversely affected by poor bone quality and can be aggravated by decortication, such as migration, loosening, or interference from surrounding tissues. However, 3D printing allows for an open fenestrated core to be incorporated in the implant design, which increases the contact area with bone and also provides an accessible route for bone integration [7,19]. Currently, the technologies in 3D-printing medical device have been developed to apply in metal and polymer materials [20]; however, the polymer materials have been considered that have some problems such as poor implant strength, damage to soft tissue, and development of inflammatory reactions leading to osteolysis. The literatures also indicated that polyetheretherketone (PEEK) has been shown to be poor osseointegration [21–23]. Porosity titanium implant have been shown excellent osseointegration property, and therefore we choose the 3D printed titanium technology to create our anchors. In addition, our threadless anchor is made of Ti6Al4V ELI powder that has been satisfied the requirements of ASTM F3001-14 which is relevant to medical devices and recognized by US FDA. In this study, we compared the primary fixation stability of a novel threadless 3D-printed suture anchor against a commercially available threaded suture anchor.

While the pullout strength of threaded suture anchors has been assessed in previous studies [11,17,19,24], research has indicated that the pullout strength weakens considerably with a larger angle between the load direction and long-axis of the anchor [17,24]. This was also evident from the results of this study whereby inserting the threaded suture anchor at 135° gave a greater pullout strength than the 90° insertion angle. However, the opposite was found for the threadless anchor, in that the smaller 90° insertion angle provided a greater pullout strength than the anchors inserted at 135°. Similar results were reported by Nagamoto et al. [14], who found that a 90° insertion angle provided the greatest pullout strength for a titanium metal threadless anchor. The static pullout strength of the threadless anchor was also significantly higher than the threaded anchor when both were inserted at 90°. However, when using a 135° insertion angle, the threaded anchor had a superior pullout strength, although the difference was not significant.

The initial pullout resistance is primarily influenced by friction generated by the axial component of the applied force. Most commercially available threaded anchors have a smooth surface and so the resistance capability is related to the thread design. However, the 3D printed anchor with rectangular cross-section generates friction through the surface

roughness and the press-fit force. When the pullout force was aligned normally with the long axis of the anchor (90° insertion angle), the threadless anchor had a better initial stability than the threaded anchor, with the resistance to pullout mainly arising from the overall contact area and the press-fit force of the rectangular shape to reduce movement or tilting. The maximum displacement (structural stiffness) of the threadless anchor was less than the threaded anchor for the 90° insertion angle, demonstrating its resistance to tilting and migration.

No failures were reported for the threadless anchor constructs with a 90° insertion angle, but the threaded anchors showed signs of gross loosening after about 21–30 cycles. For the 135° angle, the two anchor groups showed a similar trend to failure. No displacement data were recorded during the cyclic testing, but it was noted by inspection that the threaded anchors had become more displaced from the starting position. Inserting the threaded anchor into a pre-drilled hole may not provide adequate bone purchase around the distal region of the screw, which can lead to screw loosening as the distal threads move relative to the secured shaft within the proximal block (Figure 3). We propose that using a predrilled hole increases the risk of developing a windshield-wiper effect and subsequent anchor loosening. Strauss et al. [25] indicated that fixed anchors placed under cyclic loading succumb to a windshield-wiper effect, which increases motion at the bone-anchor interface, leading to loosening. The threadless suture anchor developed for this study was fixed into a predrilled tunnel by press-fitting, generating greater friction at the bone-implant interface and thus improving the fixation strength to prevent excessive interfacial micro-motion. Excessive micro-motion at the bone-implant interface may impair long-term bone ingrowth and ongrowth [26]. Similar 3D printed threadless implants have been successfully used for sacroiliac joint fusion [27–29], and in-vivo experiments have indicated that incorporating a porous surface can improve biological fixation and implant stability [7]. By referring the previous literatures related to the processing of the selective laser melted (SLM) machine used in this study, our anchor was designed to have porosities of 70% and pore sizes of 600 µm. Fuduka et al. [30] evaluated the osteoinduction of SLM titanium implants and found the superior osteoinduction property was observed when the pore sizes were in 500 and 600 µm. By an in-vivo experiment by Taniguchi et al. [31], it indicated that the Ti6Al4V device with porosity of 65% and pore size of 600 µm had more comparable mechanical strength with the bone and significant bone ingrowth than those with pore size of 300 or 900 µm.

Overall, the 3D printed suture anchor presented in this study has the potential to improve initial implant stability and long-term fixation, demonstrated by the significantly greater pullout strength and implant stiffness at a 90° insertion angle. According to our results, the greatest pullout strength for the threadless anchor occurred at a 90° insertion angle, and therefore we would recommend surgeons to maintain this angle when using threadless anchors. Because our threadless anchor is prototype, we only evaluated the feasibility of pullout and stability performance of our threadless anchor as our pilot study. Further studies including the mechanical and biocompatibility tests (cytotoxicity test, sensitization test, intracutaneous irritation test, etc.) according to ASTM and ISO standards respectively shall be performed to validate the design in this study.

The current study has some limitations to be considered. Synthetic bone blocks are intended to replicate the properties of bone, but cannot truly represent the anisotropic and viscoelastic material properties of human bone. However, synthetic bone does have some notable advantages, including negligible inter-specimen variability, low cost, readily available, and minimal specimen preparation. The use of synthetic bone compliments the aims of this study to compare the pullout properties of different suture anchors [11,19,24]. It should also be recognized that this study only used one commercially available suture anchor for comparison against the novel 3D printed threadless anchor. Future studies should consider a wider range of anchor designs. Regarding the test setup, the loading conditions applied in this study did not accurately represent physiological loading, and the models did not account for the mechanical environment at a specific repair site or

using different implantation methods. In addition, the characteristics of the sawbone post-testing were not presented in this study because the failure region is irregular and not easy to quantify. Future work may consider methods for evaluating the sawbone samples to further assess anchor loosening and associated failure modes. The 90° and 135° implantation angles are also two potential angles for application, but a wider range of angles under different conditions should be considered in follow-up studies.

5. Conclusions

The novel threadless suture anchor presented in this study had a significantly greater pullout strength and stiffness than the threaded anchor when inserted at 90°, while the two anchors had comparable results when inserted at 135°. In addition, while it has not been assessed in this study, the fixation strength of the porous 3D printed structure would likely increase over time as the bone integration process develops, improving the long-term viability of the suture anchor.

Author Contributions: Conceptualization, Y.-Y.H., L.-C.W. and C.-J.C.; methodology, F.-Y.T., L.-C.W. and Y.-Y.H.; project administration, C.-H.C. and C.-J.C.; resources, C.-H.C. and L.-C.W.; validation, F.-Y.T., C.-H.C. and C.-J.C.; writing—original draft, Y.-Y.H.; writing—review and editing, Y.-Y.H., L.-C.W. and C.-J.C. All authors have read and agreed to the published version of the manuscript.

Funding: This research received no external funding.

Institutional Review Board Statement: Not applicable.

Informed Consent Statement: Not applicable.

Data Availability Statement: We excluded this statement since all relevant data are within the manuscript.

Conflicts of Interest: The authors declare no conflict of interest.

References

- Green, J.L.; Ruppert, D.; Glisson, R.; Ibrahim, M.; Gall, K.; Levinson, H.; Ibrahim, M. Application of a novel suture anchor to abdominal wall closure. *Am. J. Surg.* **2019**, *218*, 1–6. [[CrossRef](#)]
- Visscher, L.E.; Jeffery, C.; Gilmour, T.; Anderson, L.; Couzens, G. The history of suture anchors in orthopaedic surgery. *Clin. Biomech.* **2019**, *61*, 70–78. [[CrossRef](#)] [[PubMed](#)]
- Philippon, M.J.; Faucet, S.C.; Briggs, K.K. Arthroscopic Hip Labral Repair. *Arthrosc. Tech.* **2013**, *2*, e73–e76. [[CrossRef](#)] [[PubMed](#)]
- Silver, M.D.; Daigneault, J.P. Symptomatic interarticular migration of glenoid suture anchors. *Arthrosc. J. Arthrosc. Relat. Surg.* **2000**, *16*, 102–105. [[CrossRef](#)]
- Kaar, T.; Schenck, R.C.; Wirth, M.A.; Rockwood, C.A. Complications of metallic suture anchors in shoulder surgery. *Arthrosc. J. Arthrosc. Relat. Surg.* **2001**, *17*, 31–37. [[CrossRef](#)] [[PubMed](#)]
- Djurasovic, M.; Marra, G.; Arroyo, J.S.; Pollock, R.G.; Flatow, E.L.; Bigliani, L.U. Revision Rotator Cuff Repair: Factors Influencing Results. *J. Bone Jt. Surg. -Am. Vol.* **2001**, *83*, 1849–1855. [[CrossRef](#)]
- MacBarb, R.F.; Lindsey, D.P.; Woods, S.A.; Lalor, P.A.; Gundanna, M.I.; Yerby, S.A. Fortifying the Bone-Implant Interface Part 2: An In Vivo Evaluation of 3D-Printed and TPS-Coated Triangular Implants. *Int. J. Spine Surg.* **2017**, *11*, 16. [[CrossRef](#)]
- Patel, V.; Kovalsky, D.; Meyer, S.C.; Chowdhary, A.; Lockstadt, H.; Techy, F.; Langel, C.; Limoni, R.; Yuan, P.S.; Kranenburg, A.; et al. Prospective Trial of Sacroiliac Joint Fusion Using 3D-Printed Triangular Titanium Implants. *Med. Devices Evid. Res.* **2020**, *13*, 173–182. [[CrossRef](#)]
- Wei, W.; Ali, K.; Yang, H.; Nassab, R.; Shahriyari, F.; Akpek, A.; Guan, X.; Liu, Y.; Taranejoo, S.; Tamayol, A.; et al. 3D Printed Anchoring Sutures for Permanent Shaping of Tissues. *Macromol. Biosci.* **2017**, *17*, 1700304. [[CrossRef](#)] [[PubMed](#)]
- Ntalos, D.; Huber, G.; Sellenschloh, K.; Saito, H.; Püschel, K.; Morlock, M.M.; Frosch, K.H.; Klatte, T.O. All-suture anchor pullout results in decreased bone damage and depends on cortical thickness. *Knee Surg. Sports Traumatol. Arthrosc.* **2020**, *29*, 2212–2219. [[CrossRef](#)]
- Barber, F.A.; Hapa, O.; Bynum, J.A. Comparative Testing by Cyclic Loading of Rotator Cuff Suture Anchors Containing Multiple High-Strength Sutures. *Arthrosc. J. Arthrosc. Relat. Surg.* **2010**, *26*, S134–S141. [[CrossRef](#)]
- Bynum, C.K.; Lee, S.; Mahar, A.; Tasto, J.; Pedowitz, R. Failure Mode of Suture Anchors as a Function of Insertion Depth. *Am. J. Sports Med.* **2005**, *33*, 1030–1034. [[CrossRef](#)]
- De Carli, A.; Vadalà, A.; Monaco, E.; Labianca, L.; Zanzotto, E.; Ferretti, A. Effect of Cyclic Loading on New Polyblend Suture Coupled with Different Anchors. *Am. J. Sports Med.* **2005**, *33*, 214–219. [[CrossRef](#)] [[PubMed](#)]
- Nagamoto, H.; Yamamoto, N.; Itoi, E. Effect of anchor threads on the pullout strength: A biomechanical study. *J. Orthop.* **2018**, *15*, 878–881. [[CrossRef](#)]

15. Nagamoto, H.; Yamamoto, N.; Sano, H.; Itoi, E. A biomechanical study on suture anchor insertion angle: Which is better, 90° or 45°? *J. Orthop. Sci.* **2017**, *22*, 56–62. [[CrossRef](#)] [[PubMed](#)]
16. Tingart, M.J.; Bouxsein, M.L.; Zurakowski, D.; Warner, J.P.; Apreleva, M. Three-dimensional distribution of bone density in the proximal humerus. *Calcif. Tissue Int.* **2003**, *73*, 531–536. [[CrossRef](#)]
17. Clevenger, T.A.; Beebe, M.; Strauss, E.; Kubiak, E.N. The Effect of Insertion Angle on the Pullout Strength of Threaded Suture Anchors: A Validation of the Deadman Theory. *Arthrosc. J. Arthrosc. Relat. Surg.* **2014**, *30*, 900–905. [[CrossRef](#)]
18. Liporace, F.A.; Bono, C.M.; Caruso, S.A.; Weiner, B.; Penny, K.; Feldman, A.J.; Grossman, M.G.; Haher, T.R. The Mechanical Effects of Suture Anchor Insertion Angle for Rotator Cuff Repair. *Orthopedics* **2002**, *25*, 399–402. [[CrossRef](#)] [[PubMed](#)]
19. Barber, F.A.; Herbert, M.A. Cyclic Loading Biomechanical Analysis of the Pullout Strengths of Rotator Cuff and Glenoid Anchors: 2013 Update. *Arthrosc. J. Arthrosc. Relat. Surg.* **2013**, *29*, 832–844. [[CrossRef](#)]
20. Cho, C.-H.; Bae, K.-C.; Kim, D.-H. Biomaterials Used for Suture Anchors in Orthopedic Surgery. *Clin. Orthop. Surg.* **2021**, *13*, 287–292. [[CrossRef](#)]
21. Barber, F.A. Complications of Biodegradable Materials. *Sports Med. Arthrosc. Rev.* **2015**, *23*, 149–155. [[CrossRef](#)]
22. Noiset, O.; Schneider, Y.-J.; Marchand-Brynaert, J. Fibronectin adsorption or/and covalent grafting on chemically modified PEEK film surfaces. *J. Biomater. Sci. Polym. Ed.* **1999**, *10*, 657–677. [[CrossRef](#)]
23. Toth, J.M.; Wang, M.; Estes, B.; Scifert, J.L.; Seim, H.B.; Turner, A.S. Polyetheretherketone as a biomaterial for spinal applications. *Biomaterials* **2006**, *27*, 324–334. [[CrossRef](#)]
24. Green, R.N.; Donaldson, O.W.; Dafydd, M.; Evans, S.; Kulkarni, R. Biomechanical Study: Determining the Optimum Insertion Angle for Screw-In Suture Anchors—Is Deadman’s Angle Correct? *Arthrosc. J. Arthrosc. Relat. Surg.* **2014**, *30*, 1535–1539. [[CrossRef](#)] [[PubMed](#)]
25. Strauss, E.; Frank, D.; Kubiak, E.; Kummer, F.; Rokito, A. The Effect of the Angle of Suture Anchor Insertion on Fixation Failure at the Tendon–Suture Interface after Rotator Cuff Repair: Deadman’s Angle Revisited. *Arthrosc. J. Arthrosc. Relat. Surg.* **2009**, *25*, 597–602. [[CrossRef](#)] [[PubMed](#)]
26. Kohli, N.; Stoddart, J.C.; van Arkel, R.J. The limit of tolerable micromotion for implant osseointegration: A systematic review. *Sci. Rep.* **2021**, *11*, 1–11. [[CrossRef](#)]
27. Stuesson, B.; Kools, D.; Pflugmacher, R.; Gasbarrini, A.; Prestamburgo, D.; Dengler, J. Six-month outcomes from a randomized controlled trial of minimally invasive SI joint fusion with triangular titanium implants vs. conservative management. *Eur. Spine J.* **2017**, *26*, 708–719. [[CrossRef](#)] [[PubMed](#)]
28. INSITE Study Group; Polly, D.W.; Cher, D.J.; Wine, K.D.; Whang, P.G.; Frank, C.J.; Harvey, C.F.; Lockstadt, H.; Glaser, J.A.; Limoni, R.P.; et al. Randomized Controlled Trial of Minimally Invasive Sacroiliac Joint Fusion Using Triangular Titanium Implants vs. Nonsurgical Management for Sacroiliac Joint Dysfunction. *Neurosurgery* **2015**, *77*, 674–691. [[CrossRef](#)]
29. Dengler, J.; Kools, D.; Pflugmacher, R.; Gasbarrini, A.; Prestamburgo, D.; Gaetani, P.; Cher, D.; Van Eeckhoven, E.; Annertz, M.; Stuesson, B. Randomized Trial of Sacroiliac Joint Arthrodesis Compared with Conservative Management for Chronic Low Back Pain Attributed to the Sacroiliac Joint. *J. Bone Jt. Surg.-Am. Vol.* **2019**, *101*, 400–411. [[CrossRef](#)]
30. Fukuda, A.; Takemoto, M.; Saito, T.; Fujibayashi, S.; Neo, M.; Pattanayak, D.K.; Matsushita, T.; Sasaki, K.; Nishida, N.; Kokubo, T.; et al. Osteoinduction of porous Ti implants with a channel structure fabricated by selective laser melting. *Acta Biomater.* **2011**, *7*, 2327–2336. [[CrossRef](#)]
31. Taniguchi, N.; Fujibayashi, S.; Takemoto, M.; Sasaki, K.; Otsuki, B.; Nakamura, T.; Matsushita, T.; Kokubo, T.; Matsuda, S. Effect of pore size on bone ingrowth into porous titanium implants fabricated by additive manufacturing: An in vivo experiment. *Mater. Sci. Eng. C* **2016**, *59*, 690–701. [[CrossRef](#)] [[PubMed](#)]